2005

Superconducting and Microstructural Properties of Two Types of MgB2 Films Prepared by Pulsed Laser Deposition

Y. Zhao
University of Wollongong, yue_zhao@uow.edu.au

M. Ionescu
University of Wollongong, mionescu@uow.edu.au

M. Roussel
University of Wollongong

A. V. Pan
University of Wollongong, pan@uow.edu.au

J. Horvat
University of Wollongong, jhorvat@uow.edu.au

See next page for additional authors

Superconducting and Microstructural Properties of Two Types of MgB_2 Films Prepared by Pulsed Laser Deposition

Yue Zhao, Mihail Ionescu, Marie Roussel, Alexey V. Pan, Josip Horvat, and Shi X. Dou

***Abstract*—Significant differences in superconducting and microstructural properties between two types of MgB_2 films prepared by pulsed laser deposition were determined. A very high $H_{c2} - T$ slope of 1.1 T/K was achieved in the *in situ* film. The $J_c - H$ curves of the *in situ* film also show a much weaker field dependence than that of the *ex situ* film. The magneto-optical (MO) images show that at 4 K the flux penetrates the *in situ* MgB_2 film through random paths, while for the *ex situ* film, the flux penetration pattern is mostly repeatable, indicating a defect-controlled flux penetration. Microstructural study (transmission electron microscopy and atomic force microscopy) revealed a relatively big grain size in the *ex situ* film. The correlation between the superconducting properties, microstructure and preparation conditions is discussed with regard to the two types of films.**

***Index Terms*—Magneto-optic imaging, superconducting MgB_2 films, transmission electron microscopy.**

I. Introduction

THE two-gap phonon mediated superconductor MgB_2 has some very attractive properties and great interest has been focused on the preparation of MgB_2 thin films for both theoretical and application purposes. Shortly after the discovery of superconductivity in this material, MgB_2 thin films with bulk-like T_c were achieved by *ex situ* annealing of a boron or Mg-B precursor film in Mg vapor [1], [2]. Kang and co-workers optimized the *ex situ* annealing conditions by fine-tuning the annealing temperature and time, and a very high J_c of $\sim 10^7$ A/cm^2 at 5 K, 0 T with a weak field dependence was obtained [3]. Eom and coworkers found that a high oxygen level in the MgB_2 film prepared by a two-step *ex situ* annealing procedure significantly improved the J_c in high fields [2]. Zeng *et al.* developed an *in situ* hybrid physical-chemical vapor deposition (HPCVD) method to grow high quality MgB_2 film epitaxially [4]. The J_c value of their MgB_2 film reached 3.5×10^7 A/cm^2 at 4.2 K, 0 T, but it dropped rather quickly to 10^5 A/cm^2 as the field increased to 4 T. As-grown and *in situ* annealed films, prepared by pulsed laser deposition (PLD), molecular beam epitaxy (MBE) or magneto-sputtering employing much lower substrate temperatures and shorter annealing times, generally show a small-grain feature and poor crystallization [5]–[9]. This category of films has suppressed T_c, but the J_c properties are quite good in high fields, which indicates strong pinning and intra- or inter-band scattering due to a high disorder level in the films. As can be seen, the properties of MgB_2 thin films vary significantly with different preparation processes, which are closely related to the variety of microstructures and impurity levels of those MgB_2 films. A study of this relationship could be relevant to the optimization of the film preparation.

In this paper, we report a comparative study on *in situ* and *ex situ* annealed MgB_2 films prepared by pulsed laser deposition. The relationship between the superconducting properties and the microstructure is investigated, and the influence of the preparation conditions on the two types of MgB_2 films is discussed.

II. Experimental

In the preparation of the *in situ* annealed film, the precursor film was deposited on a 250°C $Al_2O_3 - R$ substrate from a stoichiometric MgB_2 target (84% density). A pulsed excimer laser beam ($\lambda = 248$ nm) with energy fluence of 300 mJ/pulse was focused to a 8 mm^2 ellipse spot on the target. During the deposition process, the atmosphere was 120 mTorr higher purity Argon. An 800 nm Mg cap layer was deposited on top of the precursor film to compensate the Mg loss due to annealing. The film was then heated to 685°C in 12 min and kept at this temperature for 1 min in a 1 atm Ar atmosphere. For the *ex situ* annealed MgB_2 film, a boron precursor film was deposited from a boron target (~40% density) onto an $Al_2O_3 - R$ substrate in a $10^{-7} - 10^{-6}$ Torr vacuum. The precursor film was then annealed at 900°C for 30 min in a sealed stainless steel tube with Mg pellets. The details of the preparation are described in [10].

The transport measurements were carried out on a PPMS-9T magnetometer system (Quantum Design), using a standard 4-probe method and a dc current density of 1 A/cm^2. The zero-field-cooled (ZFC) magnetization vs. temperature curves and magnetization hysteresis loops of the films were measured on an MPMS-5 T magnetometer. In each measurement the applied field was perpendicular to the film plane. The J_c was calculated from the magnetization loops using the Bean model. The upper critical fields (H_{c2}) in different temperatures were obtained using 90% ρ_{Tc} points in the resistivity-temperature ($\rho - T$) curves measured in deferent fields.

The MO imaging was carried out at the University of Oslo, employing a bismuth substituted yttrium iron garnet indicator

Manuscript received October 5, 2004. This work was supported in part by Australian Research Council (ARC) under a Linkage Project (LP0219629) co-operating with Alphatech International and the Hyper Tech Research Inc.

Y. Zhao, M. Roussel, A. V. Pan, J. Horvat, and S. X. Dou are with the Institute for Superconducting and Electronic Materials, University of Wollongong, NSW 2500, Australia (e-mail: yz70@uow.edu.au).

M. Ionescu is with Australian Nuclear Science and Technology Organization (ANSTO), Australia (e-mail: mionescu@uow.edu.au).

Digital Object Identifier 10.1109/TASC.2005.848847

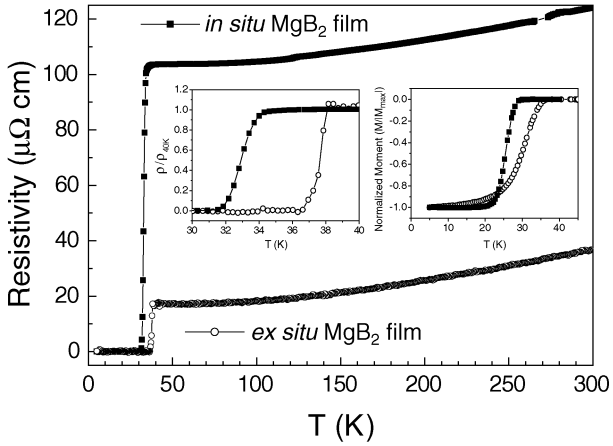

Fig. 1. Temperature dependence of the resistivity of the two types of $\mathrm{MgB_2}$ films from 5 K to 300 K in zero field. The left hand inset shows the transition curves between 30 K and 40 K. The right hand inset is the magnetization versus $\mathrm{T_c}$ curves.

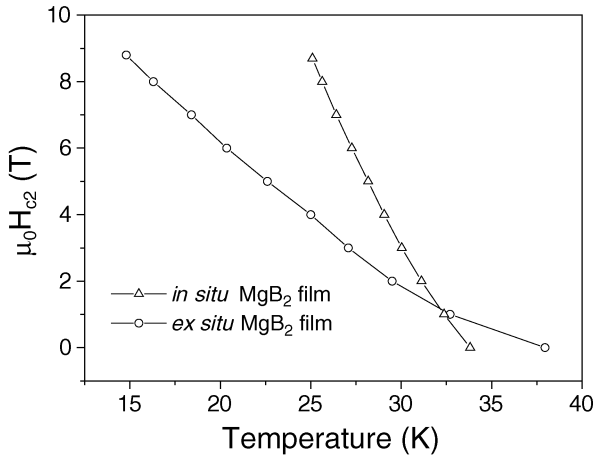

Fig. 2. Upper critical field versus temperature curves for the *in situ* and *ex situ* annealed films. The field is perpendicular to the film plane.

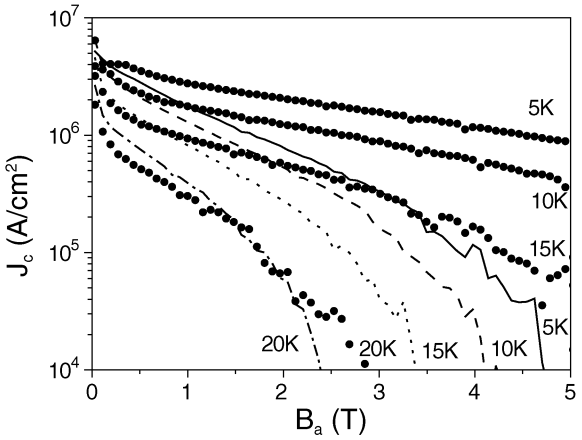

Fig. 3. Critical current of the two types of $\mathrm{MgB_2}$ films calculated from M-H loops. Circle symbols: *in situ* annealed film; lines: *ex situ* annealed film. The temperature is 5 K, 10 K, 15 K, and 20 K from top to bottom, respectively.

film [11]. The indicator film was placed directly on top of the $\mathrm{MgB_2}$ film. The magnetic field $(\mathrm{H_a})$ was applied perpendicularly to the film surface. All images were taken at a constant temperature after samples have been zero-field cooled. Transmission electron microscopy (TEM) images were taken in a 200 KV JOEL2010 TEM. The surface topography and the thickness of the films were determined by both atomic force microscopy (AFM) and scanning electron microscopy (SEM).

III. Results and Discussions

Fig. 1 shows the $\rho - \mathrm{T}$ curves of these two films. The $\mathrm{T_c}$ is 38.1 K $(\Delta \mathrm{T} = 1\ \mathrm{K})$ and 34.5 K $(\Delta \mathrm{T} = 3\ \mathrm{K})$ for the *ex situ* and *in situ* annealed films respectively. The *ex situ* annealed film has a higher $\mathrm{T_c}$ and a narrower transition width in the $\rho - \mathrm{T}$ curves. However, we notice that the bulk diamagnetism transition in the M-T curve for the *in situ* film $(\Delta \mathrm{T} = 5\ \mathrm{K})$ is actually sharper than for the *ex situ* annealed film $(\Delta \mathrm{T} = 9\ \mathrm{K})$, which indicates a more homogeneous superconducting phase in the *in situ* film, as shown in the right hand inset of Fig. 1. Also shown in Fig. 1, the resistivity value of the *in situ* annealed film is quite high, $\sim 120\ \mu\Omega \cdot \mathrm{cm}$ at 300 K, whereas the value for the *ex situ* film is as low as 36 $\mu\Omega \cdot \mathrm{cm}$. The values of the resistivity difference, $\Delta\rho_{300-40\ \mathrm{K}}$, are both 19 $\mu\Omega \cdot \mathrm{cm}$ for the two films. Since the transport property for an $\mathrm{MgB_2}$ sample is probably governed by both intra-grain scattering and inter-grain connectivity [12], [13], it is difficult to distinguish these two aspects of the influences only from the $\rho - \mathrm{T}$ curves. From a comparison of the $\rho - \mathrm{T}$ curves of our *ex situ* annealed film and a clean $\mathrm{MgB_2}$ single crystal [14], the $\Delta\rho_{300-40\ \mathrm{K}}$ of our film is about five times the value for the single crystals. If we attribute the increase of $\Delta\rho_{300-40\ \mathrm{K}}$ to a reduction of effective current carrying area by five fold, the "real" residual resistivity of our *ex situ* film should be 3.4 $\mu\Omega \cdot \mathrm{cm}$, not too far from the residual resistivity value of about 1 $\mu\Omega \cdot \mathrm{cm}$ for single crystals [14], which indicates that the *ex situ* film is fairly clean inside the $\mathrm{MgB_2}$ grains.

The stronger intra-grain scattering for the *in situ* film is revealed by the $\mathrm{H_{c2}} - \mathrm{T}$ curves for the two films shown in Fig. 2. The applied field is perpendicular to the surface of the film. Since both films do not present a grain orientation according to the AFM observation [10], the comparison of $\mathrm{H_{c2}}$ between the two films can be reliable in revealing the difference in scattering level. The slope of $\mathrm{H_{c2}} - \mathrm{T}$ for our *in situ* film is about 1.1 T/K in the temperature range from 25 K to 30 K. Employing a simple linear extrapolation, which is usually applicable for dirty $\mathrm{MgB_2}$ samples [15], the $\mathrm{H_{c2}}$ value at 0 T is estimated to be as high as 36 T. This value is significantly higher than the values of $\mathrm{H_{c2\parallel}}(0) = 21\ \mathrm{T}$ and $\mathrm{H_{c2\perp}}(0) = 7.3\ \mathrm{T}$ for the clean $\mathrm{MgB_2}$ single crystals [14], indicating a very strong scattering in our *in situ* film. The *ex situ* film shows a low $\mathrm{H_{c2}}$ slope of 0.46 T/K, attributable to a lack of intra-grain scattering, which implies that the impurity precipitates and other disorders inside the *ex situ* film are at a low level.

The field dependence of $\mathrm{J_c}$ of the two films is shown in Fig. 3. The $\mathrm{J_c}$ value of the *ex situ* film is higher than the *in situ* film, but decreases sharply with the increasing fields. Our best *in situ* annealed $\mathrm{MgB_2}$ film shows a weak field dependence of $\mathrm{J_c}$, suggesting good pinning in high fields. The $\mathrm{J_c}$ of the *in situ* film at 5 K and 5 T remains about $10^6\ \mathrm{A/cm^2}$, whereas the $\mathrm{J_c}$ for the *ex situ* film drops to less than $10^4\ \mathrm{A/cm^2}$ in the same field and temperature. The $\mathrm{J_c}$ behavior of the *ex situ* annealed $\mathrm{MgB_2}$

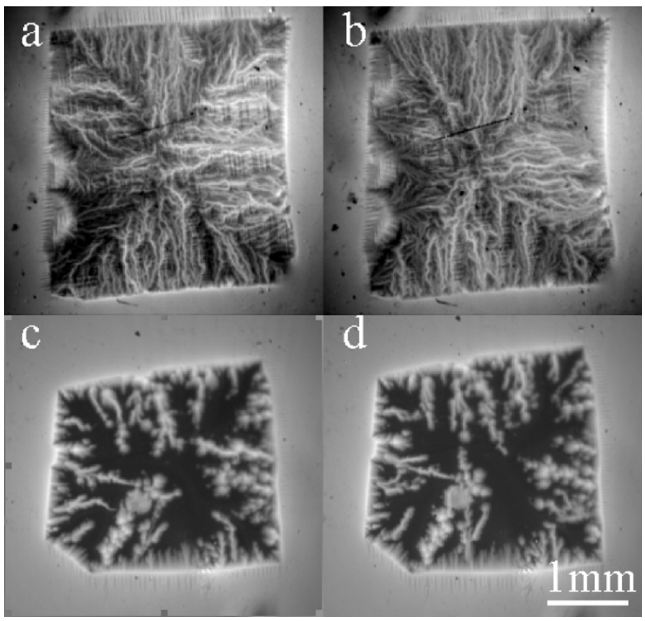

Fig. 4. MO images for the *in situ* film, shown in (a), (b) and the *ex situ* film, shown in (c), (d) at 4 K. The applied field is (a) 17 mT, 1st set of measurement, (b) 17 mT, 2nd set of measurement, (c) 25.5 mT, 1st set of measurement, and (d) 25.5 mT, 2nd set of measurement.

film is very similar to that of clean MgB_2 bulks, which lack flux pinning in high fields.

The MO images in Fig. 4 show some interesting differences in flux penetration behavior. The images correspond to a map of the out-of-plane component of the local magnetic field. The brighter the area, the stronger is the magnetic flux. At 4 K, the magnetic flux penetrates both films by abrupt avalanches. The *in situ* film shows a parallel penetration pattern from each edge of the sample, while the *ex situ* film shows a dendritic penetration. Upon inspection of Fig. 4, we find that the penetration paths in the *in situ* film are nonrepeatable in different sets of measurements. In contrast, the dendrites for the *ex situ* film is nearly identical for different set of measurements, although the development rate of each path may vary. The nonrepeatable flux avalanche at low temperature for the *in situ* film is characteristic of MgB_2 films, corresponding to thermo-magnetic instability [16]. The fact that flux penetrates the *in situ* film much further than the *ex situ* film in a same field implies an easier local heat-up for the *in situ* film, which could be attributable to a small thermal conductivity of the *in situ* film. The penetration behavior of the *ex situ* film resembles that observed in superconductors with microscopic defects, indicating defect-controlled flux jumps in the *ex situ* film. An explanation for the interesting differences found in MO observation may link the microstructural characteristics of the films to their superconducting properties.

Fig. 5 shows an AFM 3D image of the *ex situ* annealed MgB_2 film. Since the *ex situ* film has undergone a much higher annealing temperature and longer annealing time, it is reasonable to see strong crystallization after the annealing. During the grain coarsening process, the movement of the grain boundaries probably expels the disorder, such as vacancies, dislocations, impurity atoms or precipitates, from the matrix to the grain boundaries. According to the two-band phononmediated superconductivity revealed in MgB_2, the orthogonality of the electron orbitals in the two bands of MgB_2 suppresses inter-band scattering, but only the inter-band scattering has a pair-breaking effect in the two-band superconductor [12]. Intra-grain scattering usually increases the slope of H_{c2} (T) and provides flux pinning, while makes little suppression of the T_c. Thus the relatively clean MgB_2 grains in our *ex situ* film might lead to the poor J_c and H_{c2} performance. Klie *et al.* have observed the presence of $BO_x - MgO_y - BO_z$ secondary phase along grain-boundaries in MgB_2 bulk samples [17]. In some peculiar positions, such as where three big MgB_2 grains meet together, the impurities are particularly likely to concentrate, and microscopic pores could also develop at the triple junction and act as a source of cracks. Such positions are usually the thinnest part of the film as can be seen from the AFM image in Fig. 5. These thinner, nonsuperconducting, or lower T_c parts in the film may act as a preferred path for the flux penetration shown in Fig. 4(c) and (d).

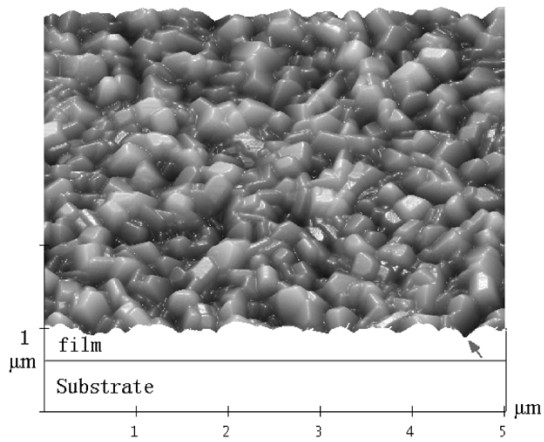

Fig. 5. AFM 3D image of the *ex situ* MgB_2 film. The surface topography shows typical randomly-oriented grains. The arrow shows a thinner part formed between two grains.

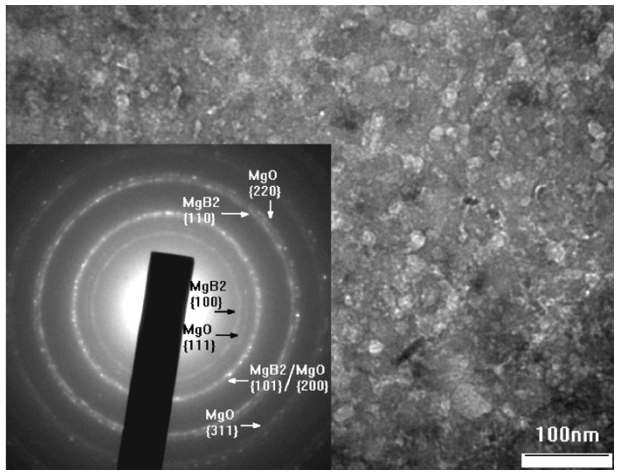

Fig. 6. TEM bright field image of a planar specimen for the *in situ* MgB_2 film. The inset is a SAD pattern from a Φ500 nm area of the film.

Fig. 6 Shows TEM and SAD pattern for the *in situ* MgB_2 film. A small-grain feature is clearly revealed by both the bright field(BF) image and the SAD ring patterns. The grain size is about 20–30 nm judging from the BF image. Strong diffraction rings from MgO also appear in the SAD image, indicating a

significant amount of MgO phase exists in the film. With the *in situ* preparation, the precursor film is deposited from a stoichiometric MgB_2 target. Thus the Mg and B atoms or clusters are finely mixed together in the precursor. The fine mixture, in turn, favors rapid MgB_2 phase formation. During the short annealing process, namely a 12 min ramping up process and a 1 min dwell at 685°C, a superconducting MgB_2 phase was formed, but a long-range diffusion is unlikely. Large amounts of disorders are probably still in their initial positions, which should be finely dispersed in the film, leading to enhanced intra-grain scattering and flux pinning, as well as an increased residual resistivity and a small thermal conductivity. The observed nano-grain structure is usually found in this type of film [6], [9]. As suggested by Bugoslavsky *et al.*, the finely distributed grain boundaries could also serve as effective pinning centers [18]. Considerable oxygen may be brought into the precursor due to magnesium's high reactivity with oxygen [2], [10]. Upon a closer look at the SAD pattern in Fig. 6, we find that the rings from MgO are constructed with distinguishable diffraction spots, while the rings from MgB_2 are more continuous, which usually indicates a larger grain size of MgO. These large MgO grains, therefore, can barely contribute to the pinning enhancement in our *in situ* film due to their unfavorable size. However, further TEM study on the distribution of oxygen with the aid of Z-contrast scanning transmission electron microscopy (STEM) and convergent-beam electron diffraction (CBED) is still necessary to clarify the role of oxygen in the *in situ* films.

IV. Conclusions

The small-grain and high-level-disorder feature of the *in situ* annealed film, which is attributable to the low annealing temperature and short annealing time, may mainly contribute to the significant improvement of flux pinning in the *in situ* MgB_2 film. In contrast, our randomly oriented *ex situ* film is probably constructed of comparatively clean grains with weak links between the grains, as a result of the annealing process which is in the grain-growing region. In accordance, defect-controlled flux jump was observed by MO imaging in our *ex situ* annealed MgB_2 film. A low temperature quick MgB_2 phase formation could be beneficial for maintaining disorder in the film, and thus of importance for high performance MgB_2 film preparation.

Acknowledgment

The authors thank T. Silver for helpful discussions. D. Wexler and Z. X. Chen provided many help and support in the TEM study.

References

[1] W. N. Kang, H.-J. Kim, E.-M. Choi, C. U. Jung, and S.-I. Lee, "Epitaxial MgB_2 superconducting thin films with a transition temperature of 39 Kelvin," *Science*, vol. 292, p. 1521, 2001.

[2] C. B. Eom *et al.*, "High critical current density and enhanced irreversibility field in superconducting MgB_2 thin films," *Nature*, vol. 411, pp. 558–560, 2001.

[3] W. N. Kang, E.-M. Choi, H.-J. Kim, H.-J. Kim, and S.-I. Lee, "Growth of superconducting MgB_2 thin films via postannealing techniques," *Physica C*, vol. 385, p. 24, 2003.

[4] X. H. Zeng *et al.*, "Superconducting MgB_2 thin films on silicon carbide substrates by hybrid physical-chemical capor deposition," *Appl. Phys. Lett.*, vol. 82, pp. 2097–2099, 2003.

[5] Y. Zhao, M. Ionescu, A. V. Pan, and S. X. Dou, "*In situ* annealing of superconducting MgB_2 films prepared by pulsed laser deposition," *Supercond. Sci. Technol.*, vol. 16, p. 1487, 2003.

[6] D. H. A. Blank *et al.*, "Superconducting Mg-B films by pulsed-laser deposition in an *in situ* two-step process using multicomponent targets," *Appl. Phys. Lett.*, vol. 79, pp. 394–396, 2001.

[7] H. M. Christen *et al.*, "Superconducting magnesium diboride films with T_c 24 K growth by pulsed laser deposition with in-situ anneal," *Physica C*, vol. 353, p. 157, 2001.

[8] K. Ueda and M. Nato, "As-grown superconducting MgB_2 thin films prepared by molecular beam epitaxy," *Appl. Phys. Lett.*, vol. 79, p. 2046, 2001.

[9] W. Jo *et al.*, "*In situ* growth of superconducting MgB_2 thin films with preferential orientation by molecular-beam epitaxy," *Appl. Phys. Lett.*, vol. 80, pp. 3563–3565, 2002.

[10] Y. Zhao, M. Ionescu, J. Horvat, and S. X. Dou, "Comparative study on in-situ and ex-situ MgB_2 Films prepared by PLD," *Supercond. Sci. Technol.*, vol. 17, pp. S482–S485, 2004.

[11] M. Roussel, A. V. Pan, Y. Zhao, S. X. Dou, and T. H. Johansen, "Flux Penetration in MgB_2 Thin Film Produced by Pulsed Laser Deposition," . Unpublished.

[12] I. I. Mazin *et al.*, "Two-gap superconductivity in MgB_2: clean or dirty?," *Phys. Rev. Lett.*, vol. 89, p. 107 002, 2002.

[13] J. M. Rowell, "The widely variable resistivity of MgB_2 samples," *Supercond. Sci. Technol.*, vol. 16, pp. R17–R27, 2003.

[14] Y. Eltsev *et al.*, "Anisotropic superconducting properties of MgB_2 single crystals probed by in-plane electrical transport measurements," *Phys. Rev. B*, vol. 65, p. R140 501, 2002.

[15] S. L. Bud'ko *et al.*, "Magnetoresistivity and $H_{c2}(T)$ in MgB_2," *Phys. Rev. B*, vol. 63, p. 220 503(R), 2001.

[16] T. H. Johansen, M. Baziljevich, D. V. Shantsev, P. E. Goa, Y. M. Gal pe rin, W. N. Kang, H. J. Kim, E. M. Choi, M.-S. Kim, and S. I. Lee, "Dendritic magnetic instability in superconducting films," *Europhys. Lett.*, vol. 59, p. 599, 2002.

[17] R. F. Klie, J. C. Idrobo, N. D. Browning, K. A. Regan, N. S. Rogado, and R. J. Cava, "Direct observation of nanometer-scale Mg- and B-oxide phases at grain boundaries in MgB_2," *Appl. Phys. Lett.*, vol. 79, pp. 1837–1839, 2001.

[18] Y. Bugoslavsky *et al.*, "Effective vortex pinning in MgB_2 thin films," *Supercond. Sci. Technol.*, vol. 15, pp. 1392–1397, 2002.